Bioorganic & Medicinal Chemistry Letters 24 (2014) 2635–2639

Contents lists available at ScienceDirect

Bioorganic & Medicinal Chemistry Letters

journal homepage: www.elsevier.com/locate/bmcl

Discovery of 5,6,7,8-tetrahydropyrido[3,4-*d*]pyrimidine inhibitors of Erk2

James F. Blake [a,*], John J. Gaudino [a], Jason De Meese [a], Peter Mohr [a], Mark Chicarelli [a], Hongqi Tian [a], Rustam Garrey [a], Allen Thomas [a], Christopher S. Siedem [a], Michael B. Welch [a], Gabrielle Kolakowski [a], Robert Kaus [a], Michael Burkard [a], Matthew Martinson [a], Huifen Chen [b], Brian Dean [b], Danette A. Dudley [b], Stephen E. Gould [b], Patricia Pacheco [b], Sheerin Shahidi-Latham [b], Weiru Wang [b], Kristina West [b], Jianping Yin [b], John Moffat [b], Jacob B. Schwarz [b]

[a] *Array BioPharma Inc, Boulder, CO 80301, USA*
[b] *Genentech Inc, 1 DNA Way, South San Francisco, CA 94080-4990, USA*

ARTICLE INFO

Article history:
Received 11 March 2014
Revised 14 April 2014
Accepted 18 April 2014
Available online 29 April 2014

Keywords:
Erk2 kinase inhibitors
Mek resistance
Structure based drug design

ABSTRACT

The discovery and optimization of a series of tetrahydropyridopyrimidine based extracellular signal-regulated kinase (Erks) inhibitors discovered via HTS and structure based drug design is reported. The compounds demonstrate potent and selective inhibition of Erk2 and knockdown of phospho-RSK levels in HepG2 cells and tumor xenografts.

Inappropriate activation of the mitogen-activated protein kinase (MAPK) signaling pathway is one of the key molecular drivers in a large number of human cancers. Overexpression of growth factor receptors and oncogenic Ras and Raf mutations, have been found in cancers of the lung, breast, colon, pancreas, skin, thyroid and blood.[1–3] Deregulation of the MAPK pathway leads to over production of phosphorylated extracellular-signal-regulated kinases, Erk1/2 (pErk), which can then activate multiple cytosolic and nuclear kinases, transcription factors and other proteins responsible for cell growth, proliferation, survival, angiogenesis and differentiation.[1,4–6]

Given the highly specific nature of the MAPK/Erk signaling pathway,[7] and its prevalence in oncogenic progression, it is not surprising that various components have proven to be attractive targets for anti-cancer drug discovery. Additionally, it has recently been shown that cells that have acquired resistance to Mek kinase inhibitors retain sensitivity to Erk inhibitors.[8] Thus there is considerable potential for Erk inhibitors to both be efficacious and to enhance/prolong efficacy in combination with inhibitors of upstream pathway components in the clinical setting.

Herein we describe the discovery and optimization of a series of selective Erk2 inhibitors that were found via combinatorial library synthesis, high throughput screening (HTS), and structure based drug design. Originally, compound **1** (Fig. 1) was synthesized as part of a combinatorial library that targeted the ATP cleft of protein kinases. The partial saturation of the bicyclic 6,6 framework and incorporation of piperidino nitrogen provides a substantially lower Clog*P* relative to the corresponding quinazoline core, which translates into significantly improved solubility properties. HTS screening identified **1** as a hit against Erk2 with an enzyme IC_{50} = 106 nM. In addition to biochemical potency in an Erk2 kinase assay, compounds were tested for their ability to inhibit phosphorylation of a downstream Erk1/2 substrate, p90Rsk in a cellular context. In vitro cellular potency of **1** was assessed by measurement of the Erk-dependent phosphorylation of p90Rsk(Ser380) levels in the HepG2 cell line (cell IC_{50} = 4.4 μM).[9]

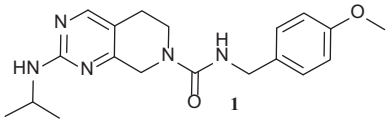

1

Figure 1. HTS hit compound **1** from combinatorial library.

* Corresponding author. Tel.: +1 303 386 1262; fax: +1 303 381 6652.
E-mail address: jblake@arraybiopharma.com (J.F. Blake).

http://dx.doi.org/10.1016/j.bmcl.2014.04.068
0960-894X/

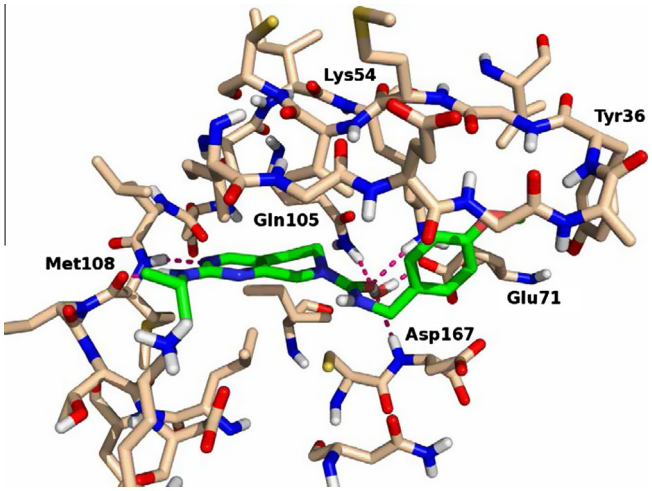

Figure 2. Compound **1** docked into the X-ray structure of Erk2.

Docking of compound **1** into an X-ray crystal structure of Erk2 suggested that the tetrahydropyridopyrimidine ring occupies the hydrophobic cavity near the hinge region (illustrated in Fig. 2). The pyrimidine ring accepts a hydrogen bond from the backbone NH of Met108 while the amino group at the 2-position donates an H-bond to the carbonyl oxygen of the same residue. Additionally, the urea oxygen of **1** accepts two hydrogen bonds, one from Lys54 and one from a bound water molecule that is complexed to Gln105, Glu71, and Asp167. The latter H-bond is a key feature of our strategy to achieve selectivity against other kinases including members of the closely related CMGC family of kinases. Based on the structure of **1** docked into Erk2, we prepared a series of substituted benzyl analogs to probe the SAR of the nascent hit.

Analogs of compound **1** were prepared according to the route outlined in Scheme 1. Primary amines **2** were initially converted to bis-CBz protected guanidines **3** using commercially available (*E*)-benzyl (1*H*-pyrazol-1-yl) methylenedicarbamate. These protected guanidines could be purified via silica gel chromatography if necessary. Deprotection gave the mono-substituted guanidines **4** which were then reacted with the enamino-ketone shown (prepared in one step from commercially available Boc-piperidin-3-one and 1-*t*-butoxy-N,N,N′,N′-tetramethylmethanediamine) to give, after Boc deprotection, a set of 2-substituted piperidinoaminopyrimidines

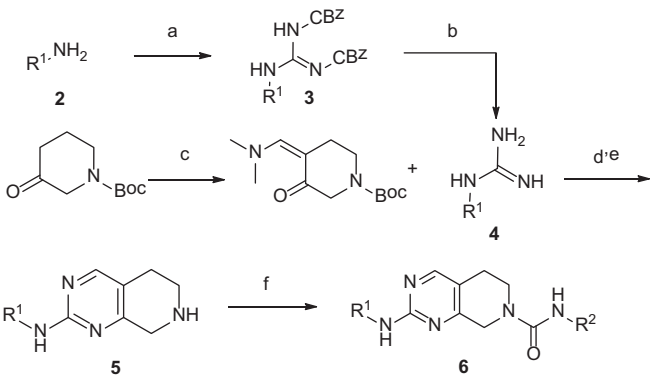

Scheme 1. Reagents and conditions: (a) **2**, (E)-benzyl (1*H*-pyrazol-1-yl)methylenedicarbamate, THF, rt, 16 h; (b) Pearlman's Catalyst, H_2 (1 atm), THF, EtOH, rt, 16 h; (c) 1-*t*-butoxy-N,N,N′,N′-tetramethylmethanediamine, toluene, rt, 16 h; (d) EtOH, NaOEt, 45 °C, 18 h; (e) 2N HCl in dioxane, CH_2Cl_2, MeOH, rt, 16 h; (f) R^2NH_2, DIEA, CDI, CH_2Cl_2, 1 h then add **5**, then 2 h, rt.

5. A final diversification step employed standard unsymmetrical urea synthesis methodology to give a set of analogs **6**.

Small hydrophobic substitution proved to afford modest potency increases while maintaining good physical properties. Both the 3-F and 3-Cl substitutions of the benzyl ring were nearly equipotent (Table 1) as were the 4-Cl and 4-F compounds. The 3-Cl, 4-F substitution yielded a slightly more cell potent lead and emerged as our starting point for further optimization efforts. This aromatic substitution pattern was also described in previous SAR for Erk2 inhibitors engaged in a similar interaction with the P-loop of the kinase.[10]

Results from docking studies and SAR from previous efforts[10] suggested that substitution of the benzylic carbon could access nearby residues such as Ser153, Asn154, Cys166, and Asp167 in a stereospecific fashion. The initial SAR in this region focused on exploring primarily polar substituents. As can be seen, the incorporation of simple alcohols at the benzyl carbon (**14**–**17**) or amines (**20**–**21**) improves both the enzyme and cell potency (Table 1). Both the primary and secondary amines were well tolerated. Testing in a limited panel of 56 kinases at 100 nM concentration revealed that compound **14** inhibited (greater than 50% inhibition) Cdk2/Cyclin A, and Gsk3β. In vitro ADME revealed compound **14** possessed somewhat high predicted hepatic clearance in human and rat microsomes (CL = 9, and 46 mL/min/kg, respectively).

Substitution of the pyrimidine via the amino linker afforded an additional opportunity to improve the potency. The results of this effort are presented in Table 2. The 4-THP analog (**28**) proved to be the most potent in this series of compounds. The Cdk2 enzyme IC_{50} = 16 nM for compound **28**. Given that the most potent compounds have exceeded the sensitivity limit of the Erk2 kinase assay ([Erk2] = 2.5 nM in the assay) the apparent selectivity ratios may be significantly underestimated. Testing against a panel of 56 kinases at 100 nM concentration showed that compound **28** inhibited (greater than 50% inhibition) Cdk2/Cyclin A, Cdk5, Hipk4, and Pkcμ. Unfortunately compound **28** still possesses somewhat high predicted hepatic clearance in human and rat microsomes (CL = 11, and 31 mL/min/kg, respectively).

During our lead optimization efforts we obtained an X-ray structure of **28** bound to Erk2 at 1.95 Å resolution (Fig. 3).[12] The crystal structure confirmed that the tetrahydropyridopyrimidine core and amino substitution interacts via a pair of H-bonds to the hinge region of Erk2 at Met108. The longer methyl hydroxy side chain interacts with the carboxylate side chain of Asp167 (2.69 Å). As we posited above, a bound water molecule forms an H-bond to the urea carbonyl of **28** (3.03 Å), and also interacts with the side chain of Lys54 (2.82 Å). The 4-THP interacts with Lys114 via the ether oxygen (3.18 Å), though it appears that the bulk of the potency gain from this substituent is derived from the hydrophobic interactions in this region. The 3-Cl,4-F phenyl group occupies a small hydrophobic pocket under the P-loop that is formed when Tyr36 is displaced toward the C-helix.

In an effort to improve the pharmacokinetics of this series of compounds further we decided to explore various substitutions at the 2-position of the tetrahydropyridopyrimidine ring and benzylic carbon of the phenyl ring. The results of this SAR are summarized in Table 3. The 3,4-dichloro substitution gave rise to some of the most potent inhibitors of Erk2. However, this substitution pattern also tended to possess higher predicted human clearance, lower fold selectivity versus Cdk2 and generally higher human PPB. A key difference between the structures of Erk2 and Cdk2 in the hinge region is the presence of the larger Phe82 of Cdk2 versus Leu107 in Erk2. Targeting this residue with larger substitutions is expected to improve the selectivity of this class of compounds further. Larger groups at the 4-position of the benzyl ring tended to increase the selectivity versus. Cdk2 (e.g., –methoxy, and $-CF_3$). Interestingly, the 3-Cl,4-CN substitution of compound **42** revealed

Table 1
Tetrahydropyridopyrimidine Benzylic SAR

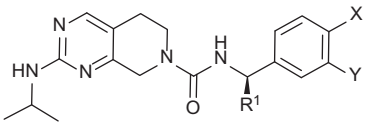

Compound	R^1	X	Y	Erk2 Inhibition IC_{50}, nM	HepG2 Cell Inhibition IC_{50}, nM
7	H	H	H	283	4384
8	H	F	H	69	6620
9	H	Cl	H	91	2138
10	H	H	F	93	2611
11	H	H	Cl	89	1856
12	H	Cl	F	81	1628
13	H	F	Cl	66	1216
14	CH_2OH	F	Cl	4	160
15	CH(*R*-CH_3)OH	F	Cl	3	88
16	CH(*S*-CH_3)OH	F	Cl	6	200
17	CH(*S*-OH)CH_2CH_3	F	Cl	2	108
18	CH_2OCH_3	F	Cl	11	368
19	$CH_2OCH_2CH_2OCH_3$	F	Cl	122	2109
20	CH_2NH_2	F	Cl	2	356
21	CH_2NHCH_3	F	Cl	4	144
22	$CH_2NHCH_2CH_2OH$	F	Cl	8	2757
23	$CH_2NHSO_2CH_3$	F	Cl	7	917

Table 2
Tetrahydropyridopyrimidine Amine SAR

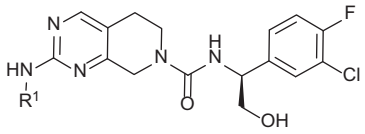

Compound	R^1	Erk2 Inhibition IC_{50}, nM	HepG2 Cell Inhibition IC_{50}, nM
24	CH_3	43	2255
25	CH_2CH_3	20	753
26	CH_2CH_2OH	9	2450
27	Cyclopentyl	4	330
28	4-THP	1	45
29	(*S*)-2-Propan-1-ol	3	473
30	*t*-Butyl	41	3009
31	(1*S*,3*S*)-3-Cyclopentanol	2	198
32	4-F phenyl	3	348
33	3,5-Dimethylisoxazol-4-yl	26	13238
34	Isobutyl	10	513
35	Acetyl	93	7438
36	1-Methyl-1*H*-pyrazol-4-yl	6	247
37	2-Methylpyridin-4-yl	7	445

a suprisingly significant drop in selectivity. Determination of the X-ray structure of **42** bound to Cdk2 revealed that the cyano group was able to accept an H-bond from the backbone NH of Tyr15, located on the P-loop of Cdk2. Attempting to balance the potency and PK properties of our compounds; we opted to revisit the 3-F, 4-Cl phenyl analog. Compound **38** proved to be potent with Erk2 IC_{50} = 2 nM, HepG2 cell IC_{50} = 25 nM and Cdk2 enzyme IC_{50} = 10 nM. The kinase selectivity profile of compound **38** was determined against an expanded panel of 170 kinases; apart from Erk1 and Erk2, only 2 other kinases, Cdk2/Cyclin A and PrkX, were inhibited by greater than 75% at a test concentration of 100 nM (Supplementary material).

Next, the in vivo PK of **38** was evaluated in male CD-1 mice and demonstrated that the clearance was moderate (CL = 33 mL/min/kg) at 0.5 mg/kg iv, and oral bioavailability was acceptable (F = 29%) at 2 mg/kg. More extensive PK evaluations were performed in female NCR nude mice, male SD rats, male beagle dogs, and male Cynomolgous monkeys. The results of these experiments are summarized in Table 4.

Given sufficient kinase selectivity and potency in inhibiting the intracellular signaling activity of Erk1/2, we tested compounds for their anti-proliferative activity against tumor cell lines carrying Braf (V600E) and K-Ras activating mutations. It has been shown that Mek inhibitors, which are expected to have the same mechanism of action as Erk inhibitors, arrest proliferation at the G1 checkpoint.[11] Proliferation of HCT116 (K-RasG12D) and A375 (B-RafV600E) cell lines was inhibited by **38** with EC_{50}s of 0.74 and 0.39 μM, respectively. Figure 4 shows that the anti-proliferative action of **38** on HCT116 cells was accompanied by an increase in the G1 (2N-DNA) fraction and inhibition of Erk-mediated p90Rsk Thr359/Ser363 phosphorylation.

Based upon its selectivity, overall physiochemical properties, in vivo PK profile and moderate plasma protein binding (ca. 89.5% bound in mouse, and ca. 82.4% bound to human plasma

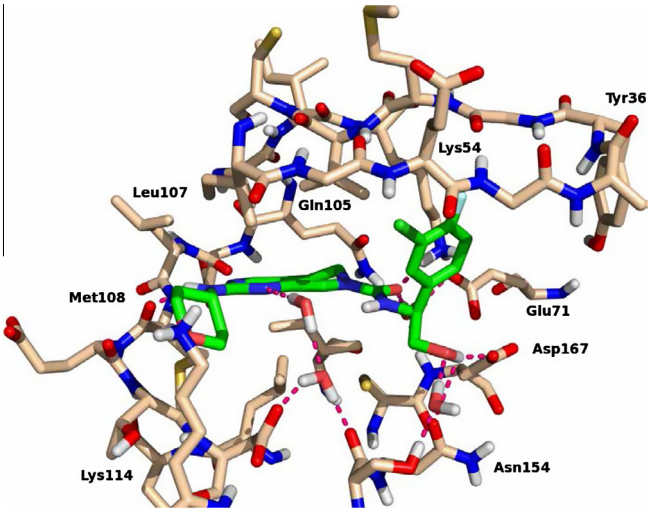

Figure 3. X-ray structure of **28** bound to Erk2, solved at 1.95 Å resolution (PDB code: 4O6E).[12]

Table 3
Tetrahydropyridopyrimidine SAR

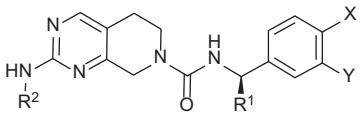

Compounds	R^1	R^2	X	Y	Erk2 Inhibition IC_{50}, nM	HepG2 Cell Inhibition IC_{50}, nM	Cdk2 Inhibition IC_{50}, nM	CL[a], mL/min/kg		Human PPB% Bound
								Rat	Human	
38	CH_2OH	4-THP	Cl	F	2	25	10	23	8	82.4
39	CH_2OH	4-THP	Cl	Cl	1	17	11	34	11	89.7
40	Me	4-THP	—CH=CH—N— (indole)		2	21	69	52	15	
41	Me	4-THP	Cl	F	1	12	13	43	13	90.5
42	Et	4-THP	CN	Cl	1	4	2	36	10	
43	Me	4*S*-(2*R*-CH_2OH-THP)	Cl	Cl	2	7	2	42	12	
44	Me	(*S*)-2-propan-1-ol	Cl	Cl	1	21	104	36	11	97.0
45	Et	(*S*)-2-propan-1-ol	F	F	3	51	13	27	7	77.4
46	Et	(*S*)-2-propan-1-ol	Cl	Cl	2	23	12	43	14	97.5
47	Me	(*S*)-2-propan-1-ol	CF_3	F	3	110	821	35	11	98.7
48	Et	(*S*)-2-propan-1-ol	OMe	Cl	2	14	71	29	8	91.9
49	Me	4-(2-methyl-pyridyl)	Cl	Cl	1	23	9	37	14	99.4
50	Me	1-methyl-1*H*-pyrazol-4-yl	Cl	Cl	1	35	4	40	17	98.2
51	Me	1-methyl-1*H*-pyrazol-5-yl	Cl	Cl	1	43	23	32	14	99.0

[a] Hepatic CL predicted from the corresponding species microsomes.

protein) we elected to advance **38** into a dose escalation PK/PD study in nude mice bearing subcutaneous human HCT116 colorectal cancer xenografts (Fig. 5).

Table 4
Key Pharmacokinetic parameters for **38**

Species	Mouse			Rat	Dog	Cyno
Dose PO (mg/kg)	30	100	150	5	2	3
C_{max} (μM)	3.12	9.82	13.9	0.09	0.59	0.16
t_{max} (h)	0.5	0.25	0.25	0.33	0.42	1.33
$t_{1/2}$ (h)	2.4	7.5	2.7	1.7	0.6	5.2
$AUC_{0\ to\ \infty}$ (μM h)	4.81	30	26.7	0.2	0.61	0.65
CL (mL/min/kg) IV[a]	134			104	32	33
F (%)	58	73	64	11	26	19

[a] IV clearance measured at 1 mg/kg.

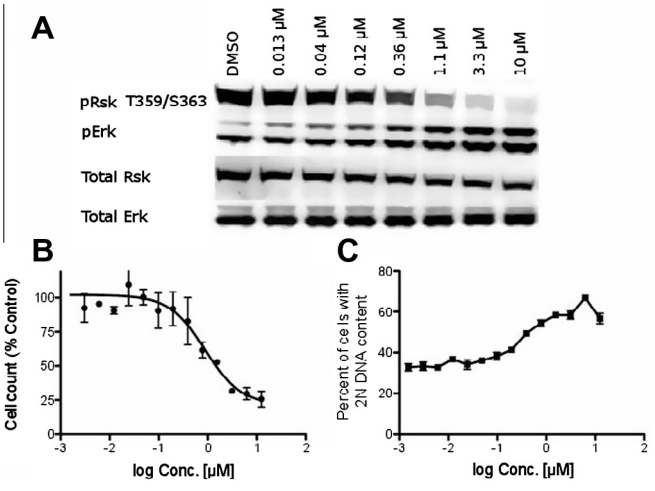

Figure 4. Activity of **38** in HCT116 cells. (A) Inhibition of Erk-mediated p90Rsk phosphorylation following treatment of cells for 2 h with the indicated concentrations of **38**. (B) Anti-proliferative activity as determined by high-content imaging following 48 h treatment. (C) Accumulation of cells with 2N DNA content as determined by high-content imaging following 48 h treatment.

At the 1 and 8 h time points the plasma levels of **38** increased in a linear fashion as the dose was increased from 75 to 150 mg/kg once daily (QD), with little increase in exposure at the 150 mg/kg twice daily (BID) dose. The corresponding pRsk knockdown at 1 h was observed to be 75–80% starting at the 75 mg/kg dose. At the 8 h time point pRsk knockdown ranged from 20% (75 mg/kg) to 55% (150 mg/kg) QD dose. Based upon these results compound **38** was progressed into a proof-of-concept tumor growth inhibition (TGI) study.

Multiple doses of **38** were administered BID by oral gavage in nude mice bearing sub-cutaneous HCT116 colorectal cancer xenografts (Fig. 6). Tumor growth inhibition of 69%, 95% CI (30, 88), was obtained with BID dosing of **38** for 28 days at 150 mg/kg. Thus, compound **38** is efficacious against human HCT116 colorectal

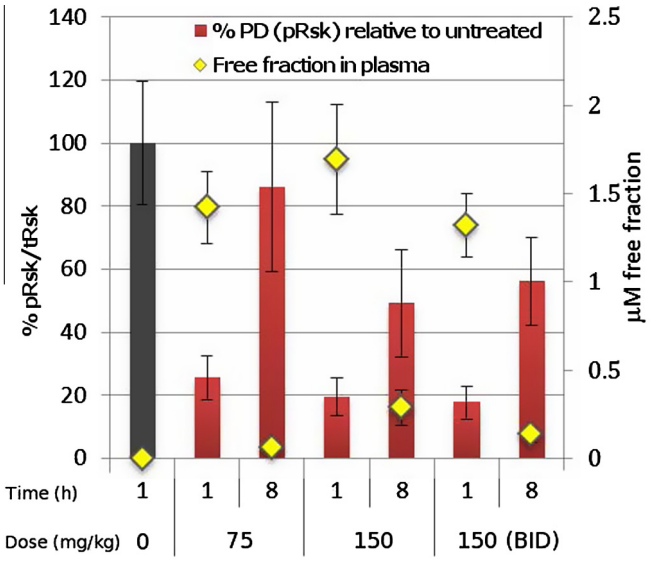

Figure 5. PK/PD in HCT116 xenograft tumors for compound **38** at 1 and 8 h time points for 75 mg/kg, 150 mg/kg, and 150 mg/kg BID in nude mice.

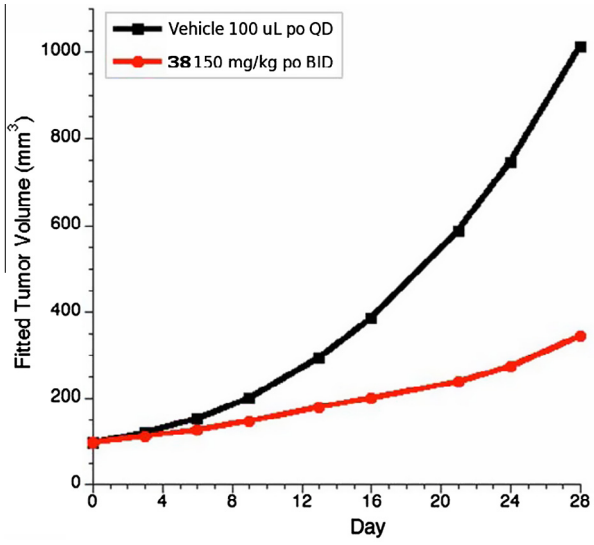

Figure 6. HCT116 colorectal tumor xenograft study for compound **38** dosed at 150 mg/kg po BID. Changes in tumor volumes over time are depicted as cubic spline fits generated via linear mixed effects analysis of log-transformed volumes.

cancer xenografts in vivo when dosed orally either QD or BID. Overall body weight loss, including the vehicle control group, was minimal (not statistically significant) in all groups. Doses of 50–150 mg/kg of **38** were generally well tolerated.

We have described the discovery and optimization of a series of potent and selective Erk2 antagonists. The compounds display potent enzyme and cell based inhibition of our primary targets. Additionally, the compounds display excellent knockdown of phosphoRsk levels in the HepG2 cell line and in human tumor xenografts. The more advanced compounds demonstrate excellent selectivity combined with good ADME properties. While this profile is encouraging, development as therapeutic agents will require additional optimization efforts.

Supplementary data

Supplementary data associated with this article can be found, in the online version, at http://dx.doi.org/10.1016/j.bmcl.2014.04.068.

References and notes

1. Dhillon, A. S.; Hagan, S.; Rath, O.; Kolch, W. *Oncogene* **2007**, *26*, 3279.
2. Platanias, L. C. *Blood* **2003**, *101*, 4667.
3. Hoshino, R.; Chatani, Y.; Yamori, T.; Tsuruo, T.; Oka, H.; Yoshida, O.; Shimada, Y.; Ari-i, S.; Wada, H.; Fujimoto, J.; Kohno, M. *Oncogene* **1999**, *18*, 813.
4. Meloche, S.; Pouyssegur, J. *Oncogene* **2007**, *26*, 3227.
5. Hanahan, D.; Weinberg, R. A. *Cell* **2000**, *100*, 57.
6. Turjanski, A. G.; Vaque, J. P.; Gutkind, J. S. *Oncogene* **2007**, *26*, 3240.
7. Roberts, P. J.; Der, C. J. *Oncogene* **2007**, *26*, 3291.
8. Hatzivassiliou, G.; Liu, B.; O'Brien, C.; Spoerke, J. M.; Hoeflich, K. P.; Haverty, P. M.; Soriano, R.; Forrest, W. F.; Heldens, S.; Chen, H.; Toy, K.; Ha, C.; Zhou, W.; Song, K.; Friedman, L. S.; Amler, L. C.; Hampton, G. M.; Moffat, J.; Belvin, M.; Lackner, M. R. *Mol. Cancer Ther.* **2012**, *11*, 1143.
9. Dalby, K. N.; Morrice, N.; Caudwell, F. B.; Avruch, J.; Cohen, P. *J. Biol. Chem.* **1998**, *273*, 1496.
10. Aronov, A. M.; Baker, C.; Bemis, G. W.; Cao, J.; Chen, G.; Ford, P. J.; Germann, U. A.; Green, J.; Hale, M. R.; Jacobs, M.; Janetka, J. W.; Maltais, F.; Martinez-Botella, G.; Namchuk, M. N.; Straub, J.; Tang, Q.; Xie, X. *J. Med. Chem.* **2007**, *50*, 1280.
11. Gysin, S.; Lee, S.-H.; Dean, N. M.; McMahon, M. *Cancer Res.* **2005**, *65*, 4870.
12. Atomic coordinates of the structure **28** bound to Erk2 were deposited with the RCSB Protein Data Bank (PDB) under the accession code 4O6E. See Supplementary material for methods.